

Solution to the many-body problem in one point

This content has been downloaded from IOPscience. Please scroll down to see the full text.

2014 New J. Phys. 16 113025

(<http://iopscience.iop.org/1367-2630/16/11/113025>)

View [the table of contents for this issue](#), or go to the [journal homepage](#) for more

Download details:

IP Address: 130.120.229.69

This content was downloaded on 09/05/2017 at 15:28

Please note that [terms and conditions apply](#).

You may also be interested in:

[Approximations for many-body Green's functions: insights from the fundamental equations](#)

Giovanna Lani, Pina Romaniello and Lucia Reining

[Erratum: Solution to the many-body problem in one point \(New J. Phys. 16 113025\)](#)

J A Berger, Pina Romaniello, Falk Tandetzky et al.

[Unphysical and physical solutions in many-body theories: from weak to strong correlation](#)

Adrian Stan, Pina Romaniello, Santiago Rigamonti et al.

[Time-dependent density-functional theory for extended systems](#)

Silvana Botti, Arno Schindlmayr, Rodolfo Del Sole et al.

[Full self-consistency versus quasiparticle self-consistency in diagrammatic approaches: exactly solvable two-site Hubbard model](#)

A L Kutepov

[Dynamical screening in correlated electron systems—from lattice models to realistic materials](#)

Philipp Werner and Michele Casula

[Combining GW calculations with exact-exchange density-functional theory: an analysis of valence-band photoemission for compound semiconductors](#)

Patrick Rinke, Abdallah Qteish, Jörg Neugebauer et al.

[Existence, uniqueness, and construction of the density-potential mapping in time-dependent density-functional theory](#)

Michael Ruggenthaler, Markus Penz and Robert van Leeuwen

Erratum: Solution to the many-body problem in one point (*New J. Phys.* **16** 113025)

J A Berger, Pina Romaniello, Falk Tandetzky, Bernardo S Mendoza, Christian Brouder and Lucia Reining

Received 14 November 2014

Accepted for publication 14 November 2014

Published 28 November 2014

New Journal of Physics **16** (2014) 119601

doi:[10.1088/1367-2630/16/11/119601](https://doi.org/10.1088/1367-2630/16/11/119601)

Keywords: many-body Green's function, Kadanoff–Baym equation, GW, GW + cumulant, one-point model

Due to a typesetting error, the following figures were not reproduced correctly. In addition, in the caption of figure 3, u_{lin}^0/V should read u_{lin}^0/v



Content from this work may be used under the terms of the [Creative Commons Attribution 3.0 licence](https://creativecommons.org/licenses/by/3.0/). Any further distribution of this work must maintain attribution to the author(s) and the title of the work, journal citation and DOI.

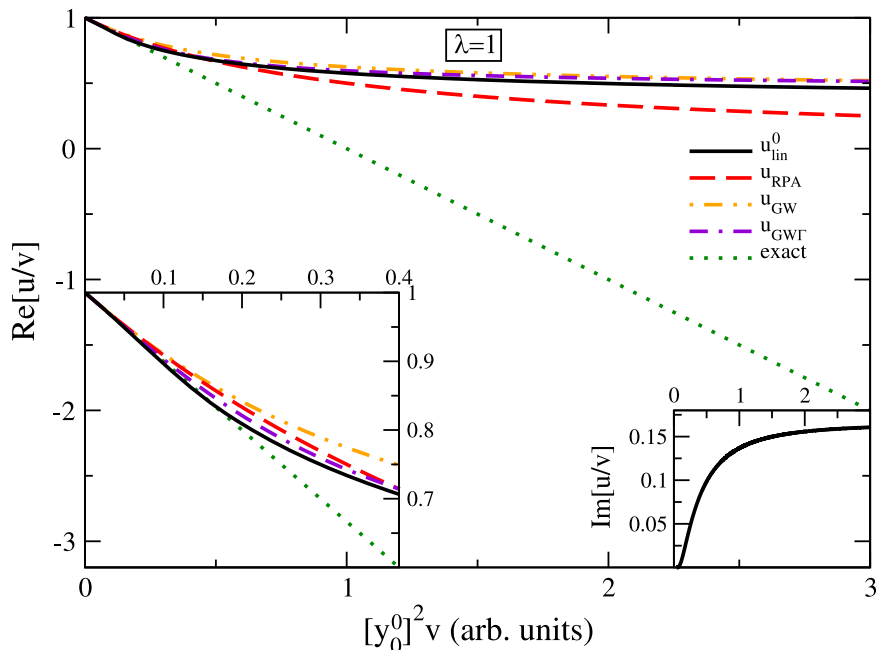


Figure 3. The real part of the screened interaction in one point u/v as a function of the interaction $[y_0^0]^2 v$ ($\lambda = 1$). Continuous line (black): u_{lin}^0/v ; dashed line (red): u_{RPA}/v ; double-dot-dashed line (orange): u_{GW}/v ; dot-double-dashed line (violet): $u_{GW\Gamma}/v$; dotted line (green): exact solution. Inset (bottom-left corner): zoom for small $[y_0^0]^2 v$. Inset (bottom-right corner): the imaginary part of u/v .

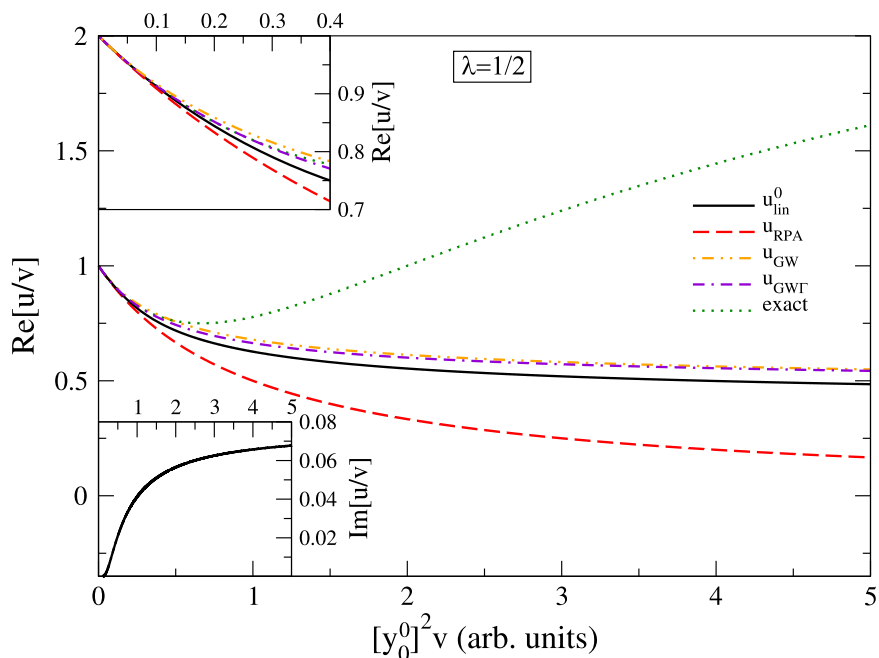


Figure 4. The real part of the screened interaction in one point u/v as a function of the interaction $[y_0^0]^2 v$ ($\lambda = \frac{1}{2}$). Continuous line (black): u_{lin}^0/y_0^0 ; dashed line (red): u_{RPA}/v ; double-dot-dashed line (orange): u_{GW}/v ; dot-double-dashed line (violet): $u_{GW\Gamma}/v$; dotted line (green): exact solution. Inset (top-left corner): zoom for small $[y_0^0]^2 v$. Inset (bottom-left corner): the imaginary part of u/v .

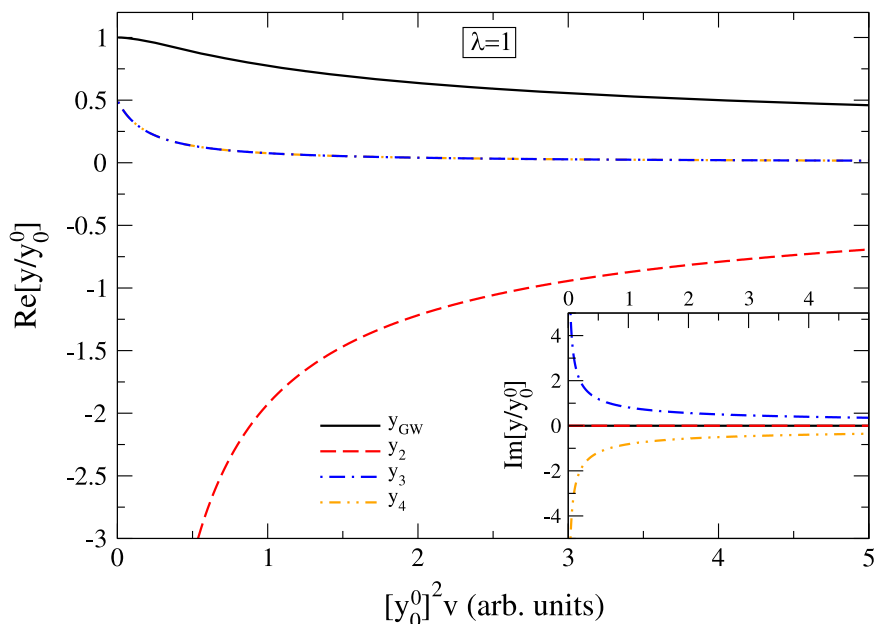


Figure 5. The real part of the GW Green's function in one point as a function of the interaction $[y_0^0]^2 v$ ($\lambda = 1$). Continuous line (black): the physical solution y_{GW}/y_0^0 ; dashed line (red): the non-physical GW solution y_2/y_0^0 ; dot-dashed line (blue): the non-physical GW solution y_3/y_0^0 ; double-dot-dashed line (orange): the non-physical GW solution y_4/y_0^0 . Inset: the imaginary part of the GW Green's function.

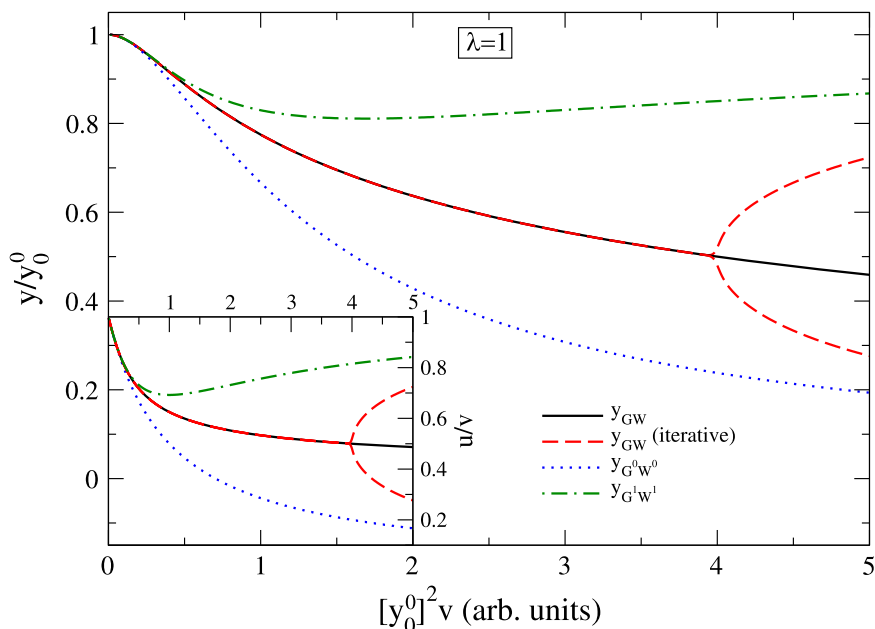


Figure 6. The GW Green's function in one point as a function of the interaction $[y_0^0]^2 v$ ($\lambda = 1$). Continuous line (black): the physical solution y_{GW}/y_0^0 ; dashed line (red): the iterative GW result (see main text for details); dotted line (blue): $y_{G^0W^0}/y_0^0$; dot-dashed line (green): $y_{G^1W^1}/y_0^0$. Inset: the screened interaction u_{GW}/v as a function of the interaction $[y_0^0]^2 v$.

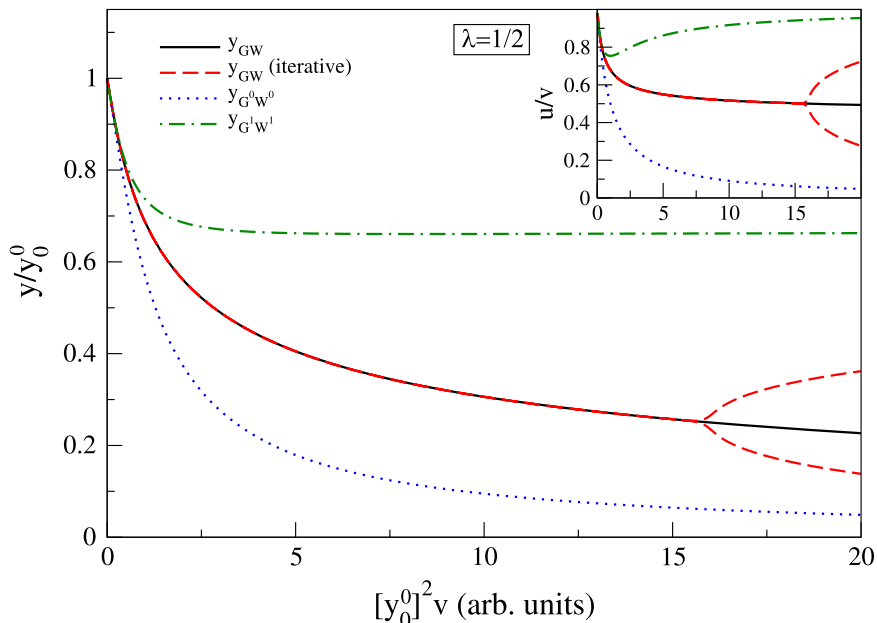


Figure 7. The GW Green's function in one point as a function of the interaction $[y_0^0]^2 v$ ($\lambda = \frac{1}{2}$). Continuous line (black): the physical solution y_{GW}/y_0^0 ; dashed line (red): the iterative GW result (see main text for details); dotted line (blue): $y_{G^0 W^0}/y_0^0$; dot-dashed line (green): $y_{G^1 W^1}/y_0^0$. Inset: the screened interaction u_{GW}/v as a function of the interaction $[y_0^0]^2 v$.

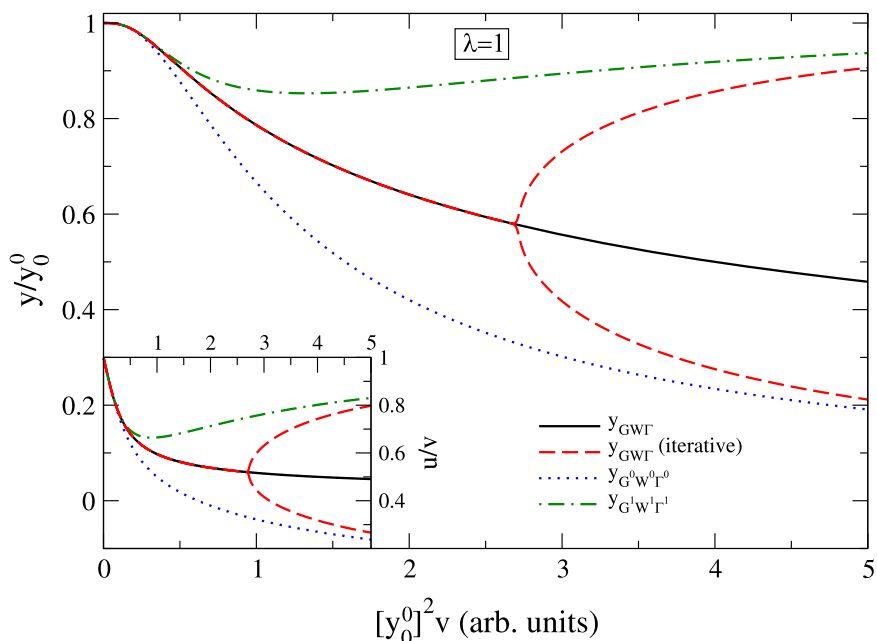


Figure 8. The GWF Green's function in one point as a function of the interaction $[y_0^0]^2 v$ ($\lambda = 1$). Continuous line (black): the physical solution y_{GWF}/y_0^0 ; dashed line (red): the iterative GWF result (see main text for details); dotted line (blue): $y_{G^0 W^0 \Gamma^0}/y_0^0$; dot-dashed line (green): $y_{G^1 W^1 \Gamma^1}/y_0^0$. Inset: the screened interaction u_{GWF}/v as a function of the interaction $[y_0^0]^2 v$.

Solution to the many-body problem in one point

J A Berger¹, Pina Romaniello², Falk Tandetzky³, Bernardo S Mendoza⁴,
Christian Brouder⁵ and Lucia Reining⁶

¹Laboratoire de Chimie et Physique Quantiques, IRSAMC, Université Toulouse III—Paul Sabatier, CNRS and European Theoretical Spectroscopy Facility (ETSF), 118 Route de Narbonne, F-31062 Toulouse Cedex, France

²Laboratoire de Physique Théorique, CNRS, IRSAMC, Université Toulouse III—Paul Sabatier and European Theoretical Spectroscopy Facility (ETSF), 118 Route de Narbonne, F-31062 Toulouse Cedex, France

³Max Planck Institute of Microstructure Physics and European Theoretical Spectroscopy Facility (ETSF), Weinberg 2, D-06120 Halle, Germany

⁴Centro de Investigaciones en Óptica, León, Guanajuato, Mexico

⁵Institut de Minéralogie, de Physique des Matériaux et de Cosmochimie, Sorbonne Universités—UPMC, Université Paris 6, UMR CNRS 7590, Muséum National d'Histoire Naturelle, IRD UMR 206, 4 place Jussieu, F-75005 Paris, France

⁶Laboratoire des Solides Irradiés, École Polytechnique, CNRS, CEA-DSM and European Theoretical Spectroscopy Facility (ETSF), F-91128 Palaiseau, France
E-mail: arjan.berger@irsamc.ups-tlse.fr

Received 26 June 2014, revised 3 September 2014

Accepted for publication 26 September 2014

Published 11 November 2014

New Journal of Physics **16** (2014) 113025

doi:[10.1088/1367-2630/16/11/113025](https://doi.org/10.1088/1367-2630/16/11/113025)

Abstract

In this work we determine the one-body Green's function as solution of a set of functional integro-differential equations, which relate the one-particle Green's function to its functional derivative with respect to an external potential. In the same spirit as Lani *et al* (2012 *New J. Phys.* **14** 013056), we do this in a one-point model, where the equations become ordinary differential equations (DEs) and, hence, solvable with standard techniques. This allows us to analyze several aspects of these DEs as well as of standard methods for determining the one-body Green's function that are important for real systems. In particular: (i) we present a strategy to determine the physical solution among the many mathematical solutions; (ii) we assess the accuracy of an approximate DE related to the *GW*+cumulant method by comparing it to the exact physical solution and to standard approximations such as *GW*; (iii) we show that the solution of the



Content from this work may be used under the terms of the [Creative Commons Attribution 3.0 licence](https://creativecommons.org/licenses/by/3.0/). Any further distribution of this work must maintain attribution to the author(s) and the title of the work, journal citation and DOI.

approximate DE can be improved by combining it with a screened interaction in the random-phase approximation. (iv) We demonstrate that by iterating the *GW* Dyson equation one does not always converge to a *GW* solution and we discuss which iterative scheme is the most suitable to avoid such errors.

Keywords: many-body Green's function, Kadanoff–Baym equation, *GW*, *GW*+cumulant, one-point model

1. Introduction

The one-body Green's function $G(\mathbf{r}\sigma t, \mathbf{r}'\sigma't')$ contains a wealth of information. Important quantities such as the density, the current density and, in particular, excitation energies such as electron removal and addition energies can be deduced from the one-body Green's function. However, to solve the equation of motion (EOM) of the one-body Green's function one requires knowledge of the two-body Green's function, the EOM of which requires knowledge of the three-body Green's function, etc. The standard procedure to cut short this chain of equations of increasing complexity is to introduce an effective potential, the self-energy, which takes into account all the many-body effects. The goal then becomes to find accurate approximations to the self-energy. Hedin proposed an iterative procedure which systematically improves the self-energy [1]. For example, one iteration of this procedure leads to the *GW* approximation. However, a second iteration already leads to a self-energy that is too complicated to be calculated for real materials.

This was one of the main motivations of Lani *et al* [2] to investigate the possibility to calculate the Green's function directly without resorting to the self-energy. The starting point for their work is the Kadanoff–Baym equation (KBE). It is a functional differential equation (DE) for the generalized one-body Green's function $G(1, 2; [\varphi])$ which is a functional of an external potential $\varphi(1)$. Here we used $(1) = (\mathbf{r}_1, \sigma_1, t_1)$ as a short-hand notation to combine the space, spin, and time variables. The equilibrium one-body Green's function is retrieved in the limit of vanishing $\varphi(1)$. The KBE is given by

$$\begin{aligned} G(1, 2; [\varphi]) = & G_0(1, 2) + \int d3 G_0(1, 3) v_H(3; [\varphi]) G(3, 2; [\varphi]) \\ & + \int d3 G_0(1, 3) \varphi(3) G(3, 2; [\varphi]) \\ & + i \int d34 G_0(1, 3) v_c(3^+, 4) \frac{\delta G(3, 2; [\varphi])}{\delta \varphi(4)}, \end{aligned} \quad (1)$$

where v_c is the Coulomb potential, G_0 is the Green's function of the noninteracting system, and

$$v_H(1; [\varphi]) = -i \int d2 v_c(1, 2) G(2, 2^+; [\varphi]) \quad (2)$$

is the Hartree potential. Furthermore, we used the notation $(1^+) = (\mathbf{r}_1, \sigma_1, t_1^+)$, where $t_1^+ = t_1 + \eta$ with $\eta \rightarrow 0^+$. All the many-body effects (exchange and correlation (xc)) beyond the Hartree potential are contained in the last term on the right-hand side of equation (1).

Solving the above functional DE for $G(1, 2; [\varphi])$ is complicated because it is a nonlinear equation in the Green's function due to the second term on the right-hand side that contains the Hartree potential which itself depends on $G[\varphi]$. Therefore, Lani *et al* approximated the KBE by linearizing this term through the replacement of the Green's function in the Hartree potential by

its first-order Taylor expansion around $\varphi = 0$ [2]. The result is a linear functional DE for $G[\varphi]$ that can be rewritten in terms of the screened Coulomb interaction $W = \epsilon^{-1}v_c$, where ϵ is the dielectric function. In order to get insights into how to solve this linearized KBE they first studied it for the one-point model. In this model there is one point in space, spin and time. Thus the functional DE becomes an ordinary DE and is easily solvable.

Below we summarize the main questions that we will answer in this work.

- What are the solutions of the full KBE in one point?
- How can we determine the physical solution and is it unique? Solving the KBE leads to a huge number of mathematical solutions. It is therefore crucial that we have a general strategy to determine the physical solution among them.
- How does the result obtained from the linearized KBE compare to the exact solution and to well-established approximations such as GW ? The linearized KBE stands at the basis of the GW +cumulant approach which has become increasingly important for the calculation of photoemission spectra [3–7]. It is therefore important to assess its accuracy.
- What is the best screened Coulomb interaction to include in the linearized KBE? The linearized KBE can be combined with several approximate screened Coulomb interactions. It is important to verify how the results depend on this choice.
- What is the best way to iterate the GW Dyson equation? The GW Dyson equation can be iterated in more than one way and it is not guaranteed that an iteration scheme will converge to the physical solution. Therefore, we will investigate which iteration schemes converge to the physical solution and which do not.

The paper is organized as follows. In section 2 we obtain the general solution of the KBE in one point and determine its physical solution. In section 3 we compare it to the solution of the linearized KBE. We compare the physical solution of the full and linearized KBE to standard approximations such as GW in section 4. In the same section we also investigate several schemes to iterate the GW equations. Finally, we summarize our conclusions in section 5.

2. KBE in the one-point model

In this section we solve the KBE and demonstrate how to find its physical solution. To transform the KBE in equation (1) to an equivalent and pertinent expression for the one-point model we use the following substitutions: $G(1, 2; [\varphi]) \rightarrow iy(z)$, $G_0(1, 2) \rightarrow iy_0^0$, $v_c(1, 2) \rightarrow iv$, and $\varphi(1) \rightarrow -iz$. As pointed out in [2] the change of prefactors compensates for the time integrals that are dropped in the one-point model. Moreover, this choice guarantees that the following constraints are satisfied when passing from the full functional problem to the one-point model: (i) since the diagonal of G is the density, i.e., $-iG(1, 1^+) = \rho(1)$, the physical solution of the KBE in one point at vanishing potential is real and nonnegative; (ii) for real, nonnegative values of v the inverse dielectric constant in the random-phase approximation (RPA) is real and has values between 0 and 1.

The KBE in one point thus becomes

$$y(z) = y_0^0 - vy_0^0 y^2(z) + y_0^0 zy(z) + vy_0^0 y'(z). \quad (3)$$

Before we discuss the general solution of equation (3) let us first determine the solution of the KBE in one point for a noninteracting system under the influence of an external potential z . The solution to this problem can be obtained by setting $\nu = 0$ in equation (3). We obtain

$$y_0(z) = \frac{y_0^0}{1 - y_0^0 z}. \quad (4)$$

In the limit of vanishing potential z this result reduces to y_0^0 as it should. It turns out that the noninteracting solution $y_0(z)$ is also a solution of equation (3) for any finite ν as can be verified by substitution. This is due to the cancelation of the two terms in equation (3) that contain ν which represent Hartree and xc contributions in one point. This cancelation is similar to what occurs for the hole part of the KBE of a one-electron system. However, we are interested in describing using a simple model some aspects of a many-electron system, for which Hartree and xc terms in equation (1) will only partially cancel. To achieve this one could, for example, study a two-point model. In this case, however, the analytical solution of the KBE is, to the best of our knowledge, out of reach. Therefore, here we propose to generalize equation (3) by introducing a parameter λ according to

$$y(z) = y_0^0 - \nu y_0^0 y^2(z) + y_0^0 z y(z) + \lambda \nu y_0^0 y'(z). \quad (5)$$

For $\lambda = 1$ we retrieve equation (3), whereas for $\lambda \neq 1$ we have partial cancelation of Hartree and xc terms. Inspired by the Hartree–Fock approximation where only like spins are affected by the exchange, we choose $\lambda = 1/2$.

We will now solve equation (5) for two values of λ ($\lambda = 1$ and $\lambda = \frac{1}{2}$) and find for each its physical solution. We will show that for $\lambda = 1$ the physical solution is indeed equal to $y_0(z)$.

2.1. Solution of the KBE in one point for $\lambda = 1$

We start by studying the case $\lambda = 1$ as it represents the KBE of equation (1) in one point. The corresponding DE is given by equation (3).

2.1.1. General solution. The general solution of equation (3) is given by

$$y_\nu(z) = y_0(z) - y_0^2(z) e^{-\frac{1}{2\nu y_0^2(z)}} \times \left[y_0(z) e^{-\frac{1}{2\nu y_0^2(z)}} + \sqrt{\frac{\pi}{2\nu}} \operatorname{erf} \left[\frac{1}{\sqrt{2\nu y_0^2(z)}} \right] - \frac{1}{C(\nu, y_0^0)} \right]^{-1}, \quad (6)$$

where $C(\nu, y_0^0)$ is function that could depend on both ν and y_0^0 . The derivation of this result can be found in appendix A.1. To emphasize that the solution depends parametrically on the interaction ν we added it as an index of y . The above result gives the complete family of exact mathematical solutions of the KBE for any external potential z .

However, obtaining the mathematical solutions of the KBE is meaningless if we would not be able to determine the function $C(\nu, y_0^0)$ that corresponds to the physical solution. It is therefore important to be able to find a strategy to obtain $C(\nu, y_0^0)$ corresponding to the physical solution that will also be applicable to the general KBE in equation (1). In the next subsection

we will present such a strategy and demonstrate that it is essential that $C(v, y_0^0)$ is independent of v .

2.1.2. Physical solution. It is a major challenge to find constraints that a physical solution should satisfy. We follow the approach of [2] and study the behavior of equation (6) in the limit of vanishing interaction, i.e., $v \rightarrow 0$. In this limit a physical solution should reduce to $y_0(z)$, the solution of the KBE for noninteracting systems, for any z . We will, as a first step, determine $C(v=0, y_0^0)$. From equation (6) we learn that for positive v and $y_0^2(z) > 0$ almost all $C(v=0, y_0^0)$ fulfill this constraint. Therefore, we will now study potentials z for which $y_0^2(z) < 0$. This can be achieved by choosing, for example, $z = (1+i)/y_0^0$. In order to study the limit $v \rightarrow 0^+$ for $y_0^2(z) < 0$ we make use of the asymptotic expansion of the error function,

$$\operatorname{erf}(z) = 1 - \frac{e^{-z^2}}{z\sqrt{\pi}} \sum_{n=0}^{\infty} (-1)^n \frac{(2n-1)!!}{(2z^2)^n}, \quad (7)$$

which is valid when $z \rightarrow \infty$ and $\operatorname{arg} z < \frac{3\pi}{4}$, to rewrite equation (6) as

$$y_v(z) = y_0(z) + \left[\frac{1}{|y_0^2(z)|} e^{-\frac{1}{2v|y_0^2(z)|}} \left(\sqrt{\frac{\pi}{2v}} - \frac{1}{C(v, y_0^0)} \right) + \frac{1}{y_0(z)} \sum_{n=1}^{\infty} (2n-1)!! (v|y_0^2(z)|)^n \right]^{-1}. \quad (8)$$

In the limit $v \rightarrow 0^+$ the second term on the right-hand side of equation (8) tends to ∞ unless $C(v=0, y_0^0) = 0$ in which case it vanishes. We conclude that $C(v=0, y_0^0) = 0$ corresponds to the physical solution.

In order to uniquely determine $C(v, y_0^0)$ for finite v we assume that $C(v, y_0^0)$ has a Taylor expansion around $v=0$. Otherwise there would be many $C(v, y_0^0)$ that fulfill the constraint that for vanishing interaction the physical solution should reduce to the noninteracting solution. Then, for $y_0^2(z) < 0$, in the limit $v \rightarrow 0^+$ the second term on the right-hand side of equation (8) tends to infinity due to the exponential function unless all the coefficients of the Taylor expansion of $C(v, y_0^0)$ vanish. In that case we obtain $y(z) = y_0(z)$ as we should. We conclude that $C(v, y_0^0) = 0$ for all v . Therefore, the physical solution is given by

$$y(z) = y_0(z) = \frac{y_0^0}{1 - y_0^0 z}. \quad (9)$$

The assumption that $C(v, y_0^0)$ has a Taylor expansion around $v=0$ is motivated by the fact that the physical result thus obtained reproduces the perturbative result, i.e., substitution of the perturbative series $\sum_{n=0}^{\infty} a_n(z)v^n$ into equation (3) and solving for the coefficients $a_n(z)$ gives back equation (9). The advantage of directly determining $C(v, y_0^0)$ corresponding to the physical solution, is that we immediately obtain the resummed result. This point will become clearer when we will discuss the case $\lambda = \frac{1}{2}$ in the next subsection.

We conclude that in the one-point model the Green's function is independent of the interaction (for $\lambda = 1$). As mentioned before, we know that in the full functional problem given

by equation (1) there is partial cancelation between Hartree and xc terms. For this reason we will now study a case for which $\lambda \neq 1$ to mimic this partial cancelation in one point.

2.2. Solution of the KBE in one point for $\lambda = \frac{1}{2}$

2.2.1. General solution. In order to have partial cancelation we now study the case $\lambda = \frac{1}{2}$. The rationale behind this choice is related to the fact that in the full functional problem given by equation (1) an important contribution to the last term is the Fock exchange. Since the prefactor of the exchange term in the Fock operator of Hartree–Fock theory is half the prefactor of the term involving the Hartree potential we chose $\lambda = \frac{1}{2}$. The resulting KBE in one point becomes

$$y(z) = y_0^0 - \nu y_0^0 y^2(z) + y_0^0 z y(z) + \frac{1}{2} \nu y_0^0 y'(z). \quad (10)$$

The solution of this DE is

$$y(z) = \left[\frac{1}{y_0(z)} + \frac{\nu y_0(z)}{2} \left(1 + \frac{y_0(z) \sqrt{\frac{\nu}{\pi}} \exp\left[-\frac{1}{\nu y_0^2(z)}\right]}{\operatorname{erf}\left[\frac{1}{\sqrt{\nu y_0^2(z)}}\right] - \frac{1}{C(\nu, y_0^0)}} \right)^{-1} \right]^{-1}. \quad (11)$$

The derivation of this result can be found in appendix A.2.

2.2.2. Physical solution. To obtain the physical solution we once again investigate $y(z)$ in the limit $\nu \rightarrow 0$. In this limit a physical solution should reduce to $y_0(z)$ for any z . We will first determine $C(\nu = 0, y_0^0)$ by studying the limit $\nu \rightarrow 0^+$ for potentials z such that $y_0^2(z) < 0$. Using the asymptotic expansion of the error function (7) we can rewrite the general solution for this case as

$$y(z) = \left[\frac{1}{y_0(z)} + \frac{\nu y_0(z)}{2} \left[1 + \left[\sqrt{\frac{\pi}{\nu}} \frac{1}{y_0(z)} e^{-\frac{1}{\nu |y_0^2(z)|}} \right. \right. \right. \\ \left. \left. \left. \times \left(1 - \frac{1}{C(\nu, y_0^0)} \right) - \sum_{n=0}^{\infty} (2n-1)!! \left(\frac{1}{2} \nu |y_0^2(z)| \right)^n \right]^{-1} \right]^{-1} \right]^{-1}. \quad (12)$$

The right-hand side of equation (12) tends to 0 in the limit $\nu \rightarrow 0^+$ unless $C(\nu = 0, y_0^0) = 0$ in which case it tends to $y_0(z)$ as it should. We conclude that $C(\nu = 0, y_0^0) = 0$ corresponds to the physical solution.

In order to uniquely determine $C(\nu, y_0^0)$ for finite ν we again assume that $C(\nu, y_0^0)$ has a Taylor expansion around $\nu = 0$. Then, for $y_0^2(z) < 0$, in the limit $\nu \rightarrow 0^+$ the right-hand side of equation (12) tends to 0 unless all the coefficients of the Taylor expansion of $C(\nu, y_0^0)$ vanish.

In that case we obtain $y(z) = y_0(z)$ as we should. We conclude that $C(v, y_0^0) = 0$ for all v . The physical solution is therefore

$$y_v(z) = \frac{2y_0(z)}{2 + vy_0^2(z)}. \quad (13)$$

It can be verified that the Taylor series of the right-hand side of equation (13) around $v = 0$ coincides with the perturbative solution of equation (10):

$$y_v(z) = y_0(z) \sum_{n=0}^{\infty} \left(-\frac{y_0^2(z)}{2} v \right)^n. \quad (14)$$

As mentioned in the previous subsection the advantage of directly determining $C(v, y_0^0)$ of the physical solution, is that we immediately obtain the resummed result (13).

We see that the physical solution (13) of the KBE in equation (10) depends on the interaction v since there is only partial cancelation between the terms involving v .

In conclusion, we have solved the KBE in one point for $\lambda = 1$ and $\lambda = \frac{1}{2}$ and we have determined the physical solution among the many mathematical solutions by demanding that it reduces to the noninteracting solution at vanishing interaction and that it does not contain nonanalytic contributions. This strategy can also be applied to the solution of the full functional problem in equation (1).

3. Quality of the linear approximation

The *GW* method is the state-of-the-art approach for calculations of quasiparticle energies and photoemission spectra [8, 9]. Recently, the *GW*+cumulant approach [3–7] has received much attention, since the photoemission spectra obtained with this method give a much better description, both qualitatively and quantitatively, of satellite peaks with respect to those obtained within the *GW* approach [4]. The *GW*+cumulant approach is based on the KBE of equation (1) in which the Hartree potential is linearized, i.e., the Hartree potential is replaced by its first-order Taylor expansion around $\varphi = 0$ [4]. It is therefore important to assess how accurate this linearized KBE is with respect to the full KBE of equation (1). Having obtained the exact physical solutions of the KBE in the one-point model we can now compare with the approximate physical solutions of the linearized KBE in one point which have been obtained in [2].

In order to keep this article self-contained as well as to introduce some quantities that will prove useful in the next section we will briefly demonstrate how one obtains the linearized KBE for the one-point model. Let us first rewrite equation (5) as

$$y(z) = y_H(z) + y_H(z)zy(z) + \lambda v y_H(z)y'(z) \quad (15)$$

in which

$$y_H(z) = y_0^0 - y_0^0 v y(z) y_H(z) = \frac{y_0^0}{1 + y_0^0 v y(z)} \quad (16)$$

represents the Hartree Green's function in one point. The linearization proposed in [2] amounts to the substitution of $y(z)$ in the above expression by its first-order Taylor expansion around

$z = 0$. This leads to

$$y_H(z) \approx \frac{y_0^0}{1 + y_0^0 v [y(z=0) + zy'(z=0)]}. \quad (17)$$

Substitution of this approximation into equation (15) results in the following linear DE for $y(z)$,

$$y(z) = y_H^0 + y_H^0 \frac{z}{e(z=0)} y'(z) + \lambda v y_H^0 y'(z) \quad (18)$$

in which

$$y_H^0 = y_H(z=0) = \frac{y_0^0}{1 + y_0^0 v y(z=0)}, \quad (19)$$

$$\frac{1}{e(z)} = 1 - vp(z), \quad (20)$$

$$p(z) = \frac{dy(z)}{dz}. \quad (21)$$

The latter two expressions represent the inverse dielectric function, and the (reducible) polarizability in one point, respectively. Introducing the change of variable,

$$\tilde{z} = \frac{z}{e(z=0)} = z(1 - vy'(z=0)), \quad (22)$$

leads to the following linear DE,

$$y(\tilde{z}) = y_H^0 + y_H^0 \tilde{z} y'(\tilde{z}) + \lambda u(\tilde{z}=0) y_H^0 y'(\tilde{z}), \quad (23)$$

where the prime in $y'(\tilde{z})$ now refers to a derivative with respect to \tilde{z} and $u(z)$ represents the screened interaction in one point. It is defined by

$$u(z) = \frac{v}{e(z)} = v(1 - vp(z)). \quad (24)$$

We note that equation (23) is not the same as the DE used in [2]. There, y_H^0 and $u(z=0)$ were assumed to be given, and independent of the interaction, whereas here we calculate them self-consistently. This also explains the different choice for the sign of the last term in our Equation (5) with respect to the corresponding equation in [2].

Using a similar strategy as before we obtain the physical solution of equation (23). It is given by

$$y_{\text{lin}}(\tilde{z}) = \sqrt{\frac{\pi}{-2\lambda u}} e^{-\frac{1}{2\lambda u} \left(\tilde{z} - \frac{1}{y_H^0} \right)^2} \left(\text{erf} \left[\frac{1}{\sqrt{-2\lambda u}} \left(\tilde{z} - \frac{1}{y_H^0} \right) \right] + 1 \right), \quad (25)$$

where $u \equiv u(\tilde{z}=0)$. Here we are mainly interested in the equilibrium solution $y_{\text{lin}}^0 = y_{\text{lin}}(\tilde{z}=0)$. For the details on how to solve equation (23) and how to find its physical solution given in equation (25) we refer the reader to [2] in which an equivalent equation to equation (23) is discussed in detail.

To compare y_{lin}^0 to the exact solutions given in equations (9) and (13) we have to express it in terms of v and y_0^0 instead of u and y_H^0 . There are two ways to achieve this. First, one can

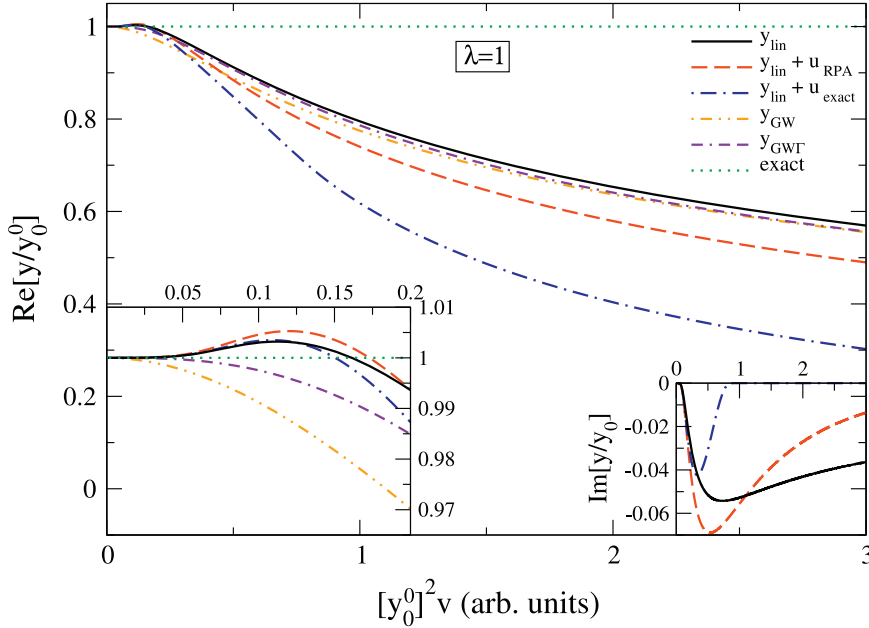


Figure 1. The real part of the Green's function in one point y_v/y_0^0 as a function of the interaction $[y_0^0]^2 v$ ($\lambda = 1$). Continuous line (black): y_{lin}^0/y_0^0 ; dashed line (red): y_{lin}^0/y_0^0 using u_{RPA} ; dot-dashed line (blue): y_{lin}^0/y_0^0 using the exact u ; double-dot-dashed line (orange): y_{GW}^0/y_0^0 ; dot-double-dashed line (violet): $y_{\text{GW}\Gamma}^0/y_0^0$; dotted line (green): exact solution. Inset (bottom-left corner): zoom for small $[y_0^0]^2 v$. Inset (bottom-right corner): the imaginary part of y_v/y_0^0 .

obtain expressions for y_{H}^0 and u that are consistent with the solution given in equation (25) by replacing $y(z=0)$ and $y'(z=0)$ in equations (19) and (24) by y_{lin}^0 and $y'_{\text{lin}}(z=0)$, respectively. The resulting expressions for y_{H}^0 and u can then be inserted into equation (25). This gives an implicit solution for y_{lin}^0 from which an explicit solution can be obtained numerically. Second, one can iterate equation (25) at $\tilde{z}=0$ together with equations (19) and (24). This leads to an explicit expression for y_{lin}^0 in terms of v and y_0^0 , provided that the iterations lead to a converged result. Both approaches lead to the same result. For the calculation of $u(z=0)$ we need $y'(z=0)$. We obtain this quantity from equation (15).

In order to numerically compare Green's functions obtained within different approximations it is convenient to plot the scaled Green's function $y(z=0)/y_0^0$ as a function of the scaled interaction $[y_0^0]^2 v$. The former is without units and for the latter we can estimate a range of values that is physically motivated; the RPA dielectric constant has typical values between 1 and ~ 10 (nonmetallic systems). Since in one point $\epsilon_{\text{RPA}} = 1 + [y_0^0]^2 v$, these values correspond to $0 \leq [y_0^0]^2 v \leq \sim 10$. Also, we note that $[y_0^0]^2 v$ corresponds to U/t of the Hubbard model in which U is the onsite interaction and t the hopping parameter, since both $[y_0^0]^2$ and $1/t$ represent a polarizability.

In figures 1 and 2 we compare y_{lin}^0/y_0^0 to the exact solution y_v/y_0^0 as a function of $[y_0^0]^2 v$ for $\lambda = 1$ and $\lambda = \frac{1}{2}$, respectively. For small values of $[y_0^0]^2 v$ the solution of the linearized KBE is nearly exact. However, the difference between y_{lin}^0 and the exact solution quickly increases with increasing v . We note that y_{lin}^0 also acquires a small imaginary part. For $\lambda = \frac{1}{2}$ the approximate

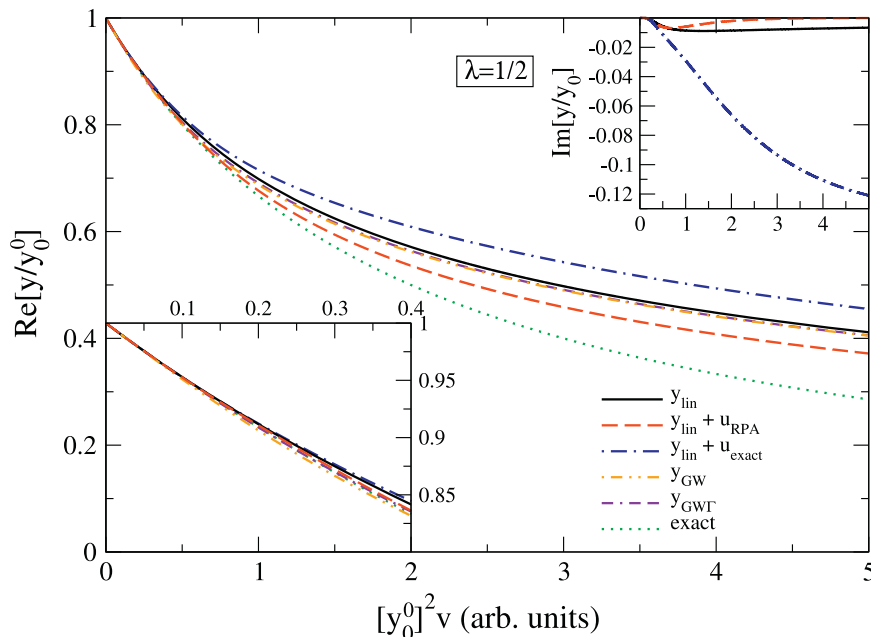


Figure 2. The real part of the Green's function in one point y_v/y_0^0 as a function of the interaction $[y_0^0]^2 v$ ($\lambda = \frac{1}{2}$). Continuous line (black): y_{lin}^0/y_0^0 ; dashed line (red): y_{lin}^0/y_0^0 using u_{RPA} ; dot-dashed line (blue): y_{lin}^0/y_0^0 using the exact u ; double-dot-dashed line (orange): y_{GW}^0/y_0^0 ; dot-double-dashed line (violet): $y_{\text{GW}\Gamma}^0/y_0^0$; dotted line (green): exact solution. Inset (bottom-left corner): zoom for small $[y_0^0]^2 v$. Inset (top-right corner): the imaginary part of y_v/y_0^0 .

solution remains much closer to the exact solution than for $\lambda = 1$. This is due to the fact that an approximation based on a screened interaction is more suitable to describe an interacting system than a noninteracting system.

In figures 1 and 2 we also report y_{lin}^0 obtained using the exact u and $u_{\text{RPA}} = \epsilon_{\text{RPA}}^{-1} v$. We see that improving the description of the screening does not necessarily improve the solutions since using the exact screening worsens the results. While for $\lambda = 1$ the results obtained with an RPA screening deteriorate with respect to y_{lin}^0 , those for $\lambda = \frac{1}{2}$ show an overall improvement when u_{RPA} is employed. We note that tendencies obtained for $\lambda = \frac{1}{2}$ should be given more weight than those obtained for $\lambda = 1$ since the former corresponds to a model of an interacting system.

In figures 3 and 4 we compare u_{lin}^0 , i.e., the screened interaction u that corresponds to y_{lin}^0 given by

$$u_{\text{lin}}^0 = v - v^2 \left. \frac{dy_{\text{lin}}(z)}{dz} \right|_{z=0}, \quad (26)$$

to the exact u for $\lambda = 1$ and $\lambda = \frac{1}{2}$, respectively. For both cases u_{lin}^0 is nearly exact for small interaction while for larger interaction it is either much too big ($\lambda = 1$) or much too small ($\lambda = \frac{1}{2}$). Also, for $\lambda = \frac{1}{2}$ the screening is qualitatively different; while the exact u/v has a minimum, u_{lin}^0/v is monotonically decreasing. We also report u_{RPA} in figures 3 and 4. While for

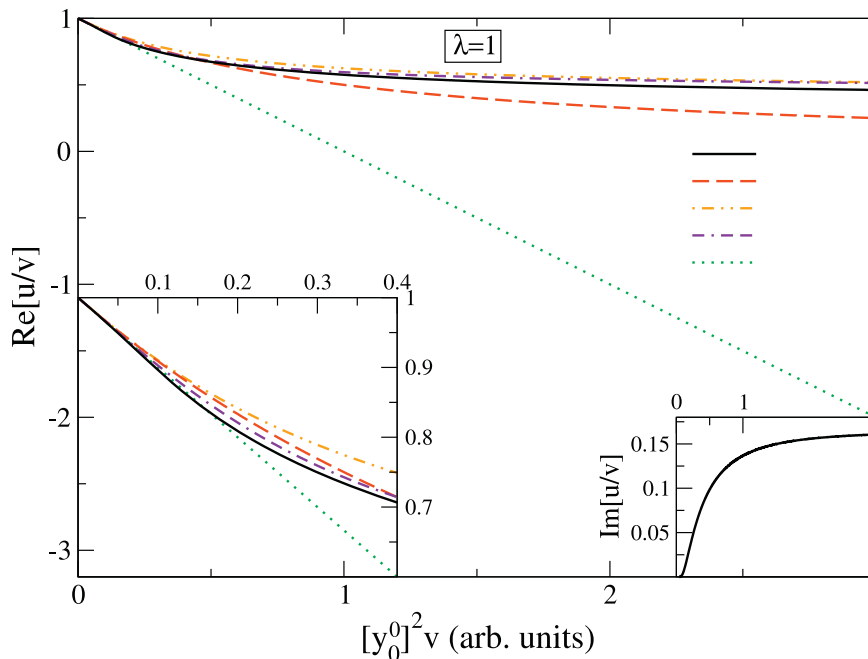


Figure 3. The real part of the screened interaction in one point u/v as a function of the interaction $[y_0^0]^2 v$ ($\lambda = 1$). Continuous line (black): u_{lin}^0/V ; dashed line (red): u_{RPA}/v ; double-dot-dashed line (orange): u_{GW}/v ; dot-double-dashed line (violet): u_{GWI}/v ; dotted line (green): exact solution. Inset (bottom-left corner): zoom for small $[y_0^0]^2 v$. Inset (bottom-right corner): the imaginary part of u/v .

$\lambda = 1$ the RPA slightly improves the screening, it deteriorates the screening for $\lambda = \frac{1}{2}$. This shows that there is a considerable cancelation of error when calculating y_{lin}^0 using u_{RPA} .

In conclusion, to obtain the best results for interacting systems the linearized KBE should be combined with an RPA screened interaction. We note that an RPA screened interaction is often used in practical calculations. For example, an RPA-type screened interaction was employed when the GW +cumulant method was applied to the description of the photo-emission spectrum of silicon leading to excellent results [4]. Also, the linearization of the KBE could be regarded as an approximation to the vertex in the self-energy expression of Hedin's equations. It is known that errors thus introduced in, for example, total energies can be partially canceled by doing a similar approximation of the vertex that appears in the expression for W [10, 11].

In order to have a better idea of the relative accuracy of y_{lin}^0 we will now compare it to some approximations obtained from Hedin's equations such as the GW approximation.

4. Solutions of Hedin's equations: GW and beyond

As mentioned in the introduction, solving the full functional problem of the KBE in equation (1) is generally considered to be a too complicated task. Therefore, a perturbative approach to obtain the one-body Green's function is usually adopted. In such an approach one defines a self-energy which contains all the many-body effects of the system, i.e., all the terms involving the

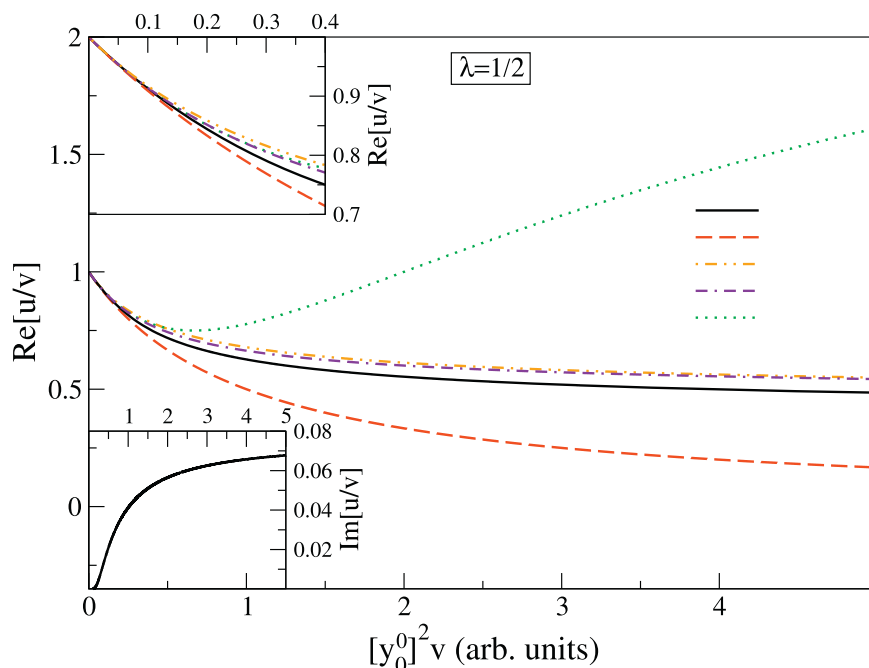


Figure 4. The real part of the screened interaction in one point u/v as a function of the interaction $[y_0^0]^2 v$ ($\lambda = \frac{1}{2}$). Continuous line (black): u_{lin}^0/y_0^0 ; dashed line (red): u_{RPA}/v ; double-dot-dashed line (orange): u_{GW}/v ; dot-double-dashed line (violet): u_{GW^I}/v ; dotted line (green): exact solution. Inset (top-left corner): zoom for small $[y_0^0]^2 v$. Inset (bottom-left corner): the imaginary part of u/v .

interaction. Here we will compare to a perturbative approach due to Hedin [1] in which the perturbation expansion is done in terms of a screened interaction instead of the bare interaction.

In one point Hedin's equations are given by

$$y(z) = y_{\text{H}}(z) + y_{\text{H}}(z)zy(z) + y_{\text{H}}(z)s_{\text{xc}}(y(z))y(z), \quad (27)$$

$$s_{\text{xc}}(y(z)) = \lambda y(z)u(z)\tilde{g}(y(z)), \quad (28)$$

$$u(z) = v - v\tilde{p}(z)u(z), \quad (29)$$

$$\tilde{p}(z) = y^2(z)\tilde{g}(y(z)), \quad (30)$$

$$\tilde{g}(y(z)) = 1 + \frac{ds_{\text{xc}}(y)}{dy}y^2(z)\tilde{g}(y(z)), \quad (31)$$

where s_{xc} is the exchange–correlation part of the self-energy in one point and $\tilde{p}(z)$ and $\tilde{g}(y(z))$ represent the irreducible polarizability and vertex function in one point, respectively. The derivation of the expressions given in equations (27)–(31) can be found in appendix B. Hedin's equations form a closed set and are equivalent to the KBE of equation (5). Hedin's equations are usually expressed for a vanishing external potential φ . Equivalent expressions can be obtained in one point by setting $z = 0$ in the above equations.

Since Hedin's equations are equivalent to the KBE, their general solution for $y(z)$ is given by equation (6) and its physical solution by equation (9) in the case $\lambda = 1$. For $\lambda = \frac{1}{2}$ the general and physical solution are given by equations (11) and (13), respectively. We can now use this

knowledge to find exact expressions for the other quantities appearing in Hedin's equations with the help of the expressions derived in appendix B. Below we summarize the results for $\lambda = 1$,

$$y(z) = \frac{y_0^0}{1 - y_0^0 z}, \quad (32)$$

$$s_{xc}(z) = \frac{vy_0^0}{1 - y_0^0 z}, \quad (33)$$

$$u(z) = v - \left(\frac{vy_0^0}{1 - y_0^0 z} \right)^2, \quad (34)$$

$$\tilde{p}(z) = \frac{[y_0^0]^2}{(1 - y_0^0 z)^2 - v[y_0^0]^2}, \quad (35)$$

$$\tilde{g}(z) = \frac{(1 - y_0^0 z)^2}{(1 - y_0^0 z)^2 - v[y_0^0]^2} \quad (36)$$

and for $\lambda = \frac{1}{2}$,

$$y(z) = \frac{2y_0^0(1 - y_0^0 z)}{b(z)}, \quad (37)$$

$$s_{xc}(z) = \frac{y_0^0 va(z)}{2(y_0^0 z - 1)b(z)}, \quad (38)$$

$$u(z) = v + 2[y_0^0]^2 v^2 \frac{a(z)}{b^2(z)}, \quad (39)$$

$$\tilde{p}(z) = -\frac{2[y_0^0]^2 a(z)}{b^2(z) + 2[y_0^0]^2 va(z)}, \quad (40)$$

$$\tilde{g}(z) = -\frac{a(z)b^2(z)}{2(1 - y_0^0 z)^2 (b^2(z) + 2[y_0^0]^2 va(z))}, \quad (41)$$

where the functions $a(z)$ and $b(z)$ are defined by

$$a(z) = v[y_0^0]^2 - 2(1 - y_0^0 z)^2, \quad (42)$$

$$b(z) = v[y_0^0]^2 + 2(1 - y_0^0 z)^2. \quad (43)$$

We see that for $\lambda = 1$ the exchange–correlation part of the self-energy $s_{xc}(z)$ is equal to minus the Hartree potential. This is a consequence of the fact that in one point the physical solution is equal to the noninteracting solution. In this case the interactions included in the Hartree potential that are implicitly contained in $y_H(z)$ are spurious. Therefore, the only purpose of $s_{xc}(z)$ is to cancel the effects of the Hartree potential. As a result the Green’s function in one point $y(z)$ becomes equal to the noninteracting Green’s function as it should.

We note that Molinari *et al* [12, 13] have studied a set of Hedin’s equations (at $z = 0$) within the one-point model that are slightly modified with respect to those presented in this section. The modification is in the irreducible polarization given in equation (30) to which they added a minus sign, i.e., $\tilde{p} = -y^2\tilde{g}$. Starting from these modified Hedin’s equations Pavlyukh and Hübner [14] found an implicit solution for the Green’s function. In appendix C we demonstrate how one can obtain an explicit solution.

In the following we will evaluate some approximations to Hedin’s equations. Since we are mainly interested in the Green’s function at vanishing external potential φ , we will only consider the case $z = 0$ in the remainder of this section.

4.1. GW

The GW approximation in one point is obtained by setting $s_{xc} = 0$ and performing one iteration of Hedin’s equations starting with the vertex function \tilde{g} . Therefore, in the GW approximation, Hedin’s equations in one point are written as

$$\tilde{g} = 1, \quad (44)$$

$$\tilde{p} = y^2, \quad (45)$$

$$u = \frac{v}{1 + vy^2}, \quad (46)$$

$$s_{xc} = \lambda \frac{vy}{1 + vy^2}, \quad (47)$$

$$y = \frac{y_H^0}{1 - y_H^0 s_{xc}} \quad (48)$$

$$= \frac{y_0^0(1 + vy^2)}{1 + (1 - \lambda)y_0^0 vy + vy^2 + y_0^0 v^2 y^3}, \quad (49)$$

where in the last step we used equation (19).

4.1.1. Exact solution. The GW Dyson equation in one point given in equation (49) can be rewritten as a quartic equation for y :

$$y_0^0 v^2 y^4 + vy^3 - \lambda y_0^0 vy^2 + y - y_0^0 = 0. \quad (50)$$

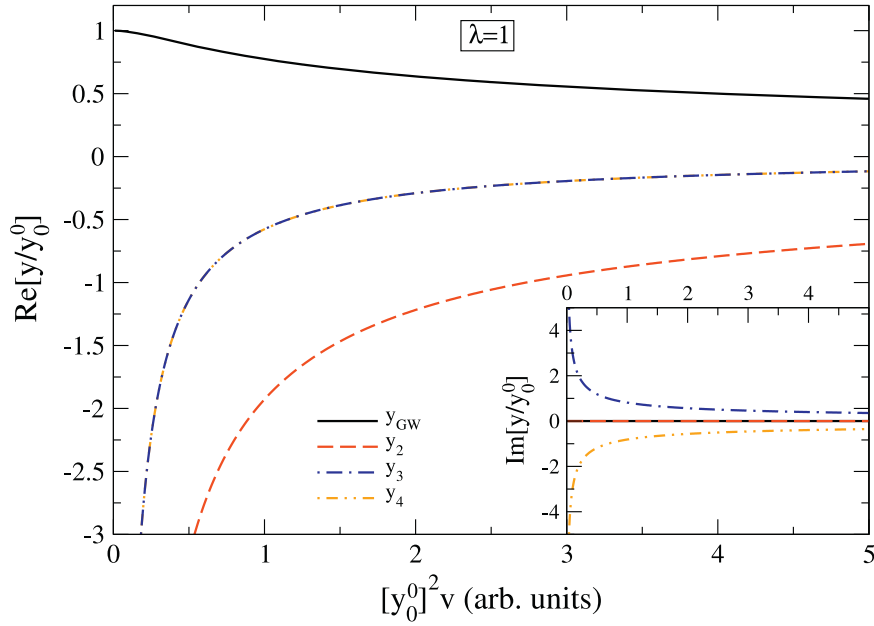


Figure 5. The real part of the GW Green's function in one point as a function of the interaction $[y_0^0]^2 v$ ($\lambda = 1$). Continuous line (black): the physical solution y_{GW}/y_0^0 ; dashed line (red): the nonphysical GW solution y_2/y_0^0 ; dot-dashed line (blue): the nonphysical GW solution y_3/y_0^0 ; double-dot-dashed line (orange): the nonphysical GW solution y_4/y_0^0 . Inset: the imaginary part of the GW Green's function.

The four solutions can be obtained analytically and are given by

$$y_{1,2} = -\frac{1}{4y_0^0 v} - S \pm \frac{1}{2} \sqrt{-4S^2 - 2r + \frac{q}{S}}, \quad (51)$$

$$y_{3,4} = -\frac{1}{4y_0^0 v} + S \pm \frac{1}{2} \sqrt{-4S^2 - 2r - \frac{q}{S}}, \quad (52)$$

where

$$r = -\frac{8\lambda [y_0^0]^2 v + 3}{8[y_0^0]^2 v^2}, \quad (53)$$

$$q = \frac{(8 + 4\lambda)[y_0^0]^2 v + 1}{8[y_0^0]^3 v^3}, \quad (54)$$

$$S = \frac{1}{2} \sqrt{-\frac{2}{3}r + \frac{1}{3y_0^0 v^2} \left(Q + \frac{4_0}{Q} \right)}, \quad (55)$$

$$Q = \left[\frac{\Delta_1 + \sqrt{\Delta_1^2 - 4\Delta_0^3}}{2} \right]^{1/3} \quad (56)$$

with

$$\Delta_0 = -3v - (12 - \lambda^2)[y_0^0]^2 v^2 \quad (57)$$

$$\Delta_1 = 9\lambda y_0^0 v^2 - (72 + 2\lambda^2)\lambda [y_0^0]^3 v^3. \quad (58)$$

We note that in [2] y_H^0 is kept fixed instead of y_0^0 and y is obtained in terms of u instead of v . As a consequence Lani *et al* only find two solutions, one physical solution and one nonphysical solution. In figure 5 we report the four solutions as a function of the scaled interaction $[y_0^0]^2 v$ for $\lambda = 1$. The physical solution is identified by verifying that in the limit $v \rightarrow 0$ the Green's function y reduces to the noninteracting Green's function y_0^0 . It is given by

$$y_{GW} = y_1 = -\frac{1}{4y_0^0 v} - S + \frac{1}{2} \sqrt{-4S^2 - 2p + \frac{q}{S}}. \quad (59)$$

The other three solutions diverge when $v \rightarrow 0$. We note that this is consistent with the first theorem derived in [15]. We obtain similar results for $\lambda = \frac{1}{2}$.

In figures 1 and 2 we compare y_{GW} to the exact physical solution of the KBE and the approximate physical solution of the linearized KBE. For $\lambda = 1$ at small interaction y_{lin}^0 is somewhat better than y_{GW} . Otherwise, we observe that the GW approximation leads to results that are generally very close to those obtained from the linearized KBE. This finding can be surprising since in the full functional problem the linearized KBE contains many more diagrams than GW . However, in the one-point model many features, such as the spectral function, for which these diagrams are important [3–7], are absent. For this reason the difference between GW and the linearized KBE cannot be detected in one point.

In figures 3 and 4 we compare the GW screened interaction u_{GW} , given by

$$u_{GW} = \frac{v}{1 + v y_{GW}^2}, \quad (60)$$

to the exact screening and to u_{lin}^0 . For $\lambda = 1$ the GW screening is slightly worse than u_{lin}^0 while in the case of $\lambda = \frac{1}{2}$ the GW screening is somewhat better than u_{lin}^0 .

4.1.2. Iterative solution. A direct solution of the full GW Dyson equation is, in general, not feasible. Therefore the GW equations are usually solved iteratively. It is important to verify that the iterative GW solution is indeed equal to the physical GW solution for all interaction strengths. Since for the one-point model we have obtained the exact physical solution we can now compare it to the iterative GW solution.

The GW Dyson equation can be rewritten in several ways and therefore many iterative schemes are possible. Let us first study the most common iteration scheme. It is given by

$$G_{n+1} = \left[G_{H,n}^{-1} - iG_n W_n \right]^{-1}, \quad (61)$$

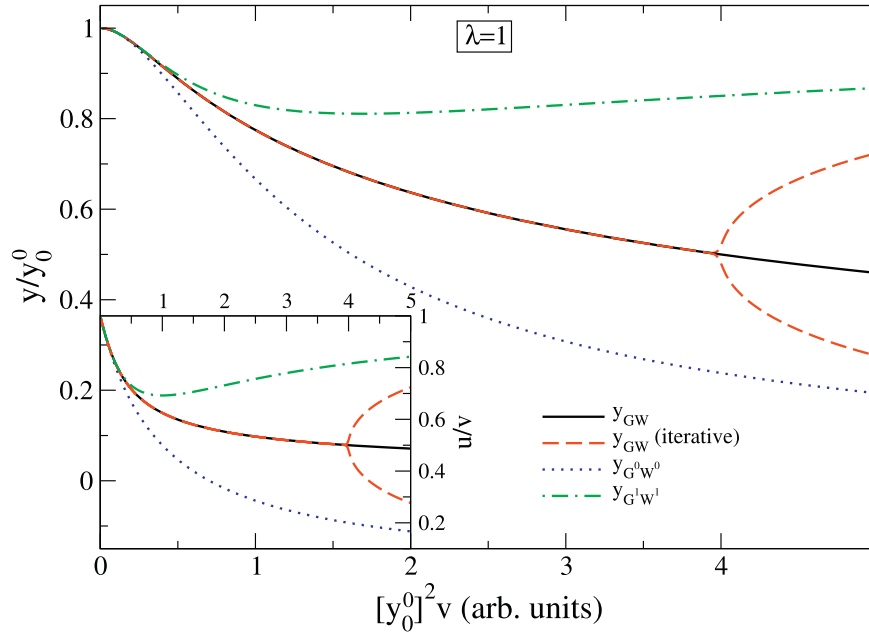


Figure 6. The *GW* Green's function in one point as a function of the interaction $[y_0^0]^2 v$ ($\lambda = 1$). Continuous line (black): the physical solution y_{GW}/y_0^0 ; dashed line (red): the iterative *GW* result (see main text for details); dotted line (blue): $y_{G^0W^0}/y_0^0$; dot-dashed line (green): $y_{G^1W^1}/y_0^0$. Inset: the screened interaction u_{GW}/v as a function of the interaction $[y_0^0]^2 v$.

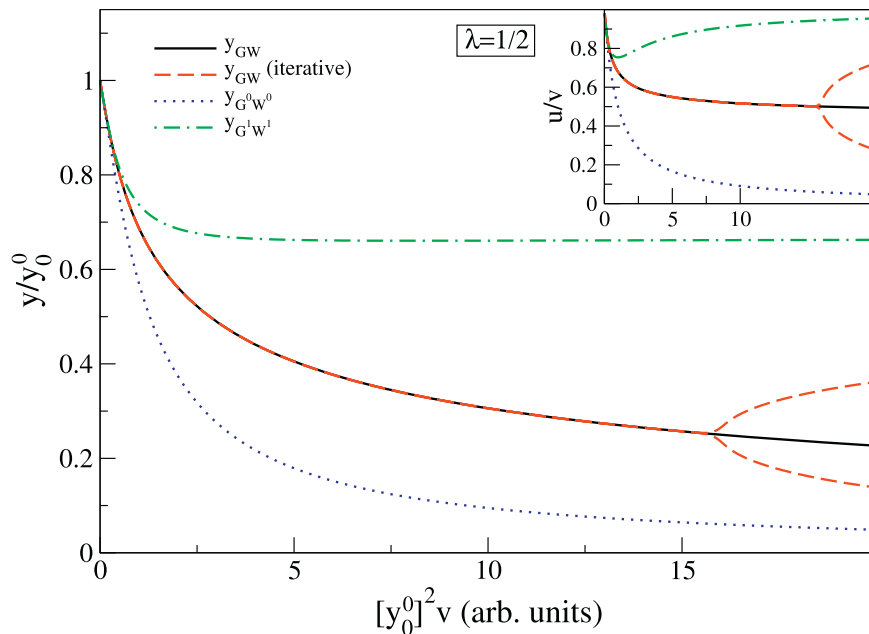


Figure 7. The *GW* Green's function in one point as a function of the interaction $[y_0^0]^2 v$ ($\lambda = \frac{1}{2}$). Continuous line (black): the physical solution y_{GW}/y_0^0 ; dashed line (red): the iterative *GW* result (see main text for details); dotted line (blue): $y_{G^0W^0}/y_0^0$; dot-dashed line (green): $y_{G^1W^1}/y_0^0$. Inset: the screened interaction u_{GW}/v as a function of the interaction $[y_0^0]^2 v$.

where the Hartree Green's function $G_{H,n}$ and the screened interaction W_n are given by

$$G_{H,n} = [1 + iG_0 v_c G_n]^{-1} G_0, \quad (62)$$

$$W_n = [1 + i v_c G_n G_n]^{-1} v_c. \quad (63)$$

In the one-point model this iteration scheme corresponds to

$$y_{n+1} = \frac{y_0^0 (1 + v y_n^2)}{1 + (1 - \lambda) y_0^0 v y_n + v y_n^2 + y_0^0 v^2 y_n^3}. \quad (64)$$

To iteratively solve Hedin's equations we start from the noninteracting solution, i.e., $y_0 = y_0^0$, followed by substitution of this expression into the right-hand side of equation (64). This leads to the first-order approximation to the GW solution,

$$y_1 \equiv y_{G^0 W^0} = \frac{y_0^0 (1 + v [y_0^0]^2)}{1 + (1 - \lambda) v [y_0^0]^2 + v [y_0^0]^2 + v^2 [y_0^0]^4}. \quad (65)$$

This result represents the $G^0 W^0$ solution in one point. By substituting the first-order result into equation (64) one obtains the second-order approximation to y_{GW} and continuation of this iteration scheme will lead to higher-order approximations to y_{GW} .

In figures 6 and 7 we compare several of these approximations to the exact GW result in one point for $\lambda = 1$ and $\lambda = \frac{1}{2}$, respectively. We see that $y_{G_0 W_0}$ is close to y_{GW} for small values of the interaction but largely underestimates it when the interaction becomes stronger. Instead, $y_{G_1 W_1}$ largely overestimates y_{GW} for large v . However, the most interesting result is that beyond a certain interaction strength, i.e., $[y_0^0]^2 v > 4/\lambda^2$, the iterative result does not converge to y_{GW} . In fact, the iterative result oscillates between two values, neither of which is equal to y_{GW} . This conclusion also holds when the starting point is chosen close to y_{GW} .

To explain the discrepancy between the exact and iterative GW result we first note that equation (64) is of the form $y = f(y)$. As a consequence y_{GW} is a fixed point of this equation, i.e., $y_{GW} = f(y_{GW})$. A fixed point is called attracting if upon iteration the result converges to y_{GW} when one starts from an initial value that lies in the vicinity of y_{GW} and it is called repelling otherwise. If $|f'(y_{GW})| < 1$ (> 1) then y_{GW} is an attracting (repelling) fixed point. It can thus be verified that y_{GW} is a repelling fixed point when $[y_0^0]^2 v > 4/\lambda^2$. This demonstrates that iteration of equation (49) for $[y_0^0]^2 v > 4/\lambda^2$ will never lead to the physical GW solution. Similarly, one can verify that y_{GW} is an attracting fixed point when $0 \leq [y_0^0]^2 v < 4/\lambda^2$. We note that this is consistent with the second theorem derived in [15].

In [2] it was shown that the solution obtained by solving the GW equations iteratively depends strongly on the iteration scheme used. In their case they solved Hedin's equations iteratively for fixed values of y_H^0 and u . This leads to two solutions of which only one is a physical solution. They showed that depending on the chosen iteration scheme the solution could be either the physical or the nonphysical solution. Here we show that, moreover, there are iteration schemes that lead to results that are not solutions at all. We also note that we have obtained this result using an iterative scheme that is equivalent to that used in most practical applications [16–18].

We obtain a different iteration scheme when, instead of writing the Dyson equation as in equation (61) we write it according to

$$G_{n+1} = G_{H,n} + iG_{H,n}G_nW_nG_n. \quad (66)$$

In the one-point model this iteration scheme corresponds to

$$y_{n+1} = \frac{y_0^0(1 + (1 + \lambda)vy_n^2)}{1 + y_0^0vy_n + vy_n^2 + y_0^0v^2y_n^3}. \quad (67)$$

One can verify that y_{GW} is an attracting fixed point of equation (67) for all v . Therefore, iteration of equation (67) is guaranteed to converge to the exact GW solution (provided that the initial value lies in the vicinity of y_{GW}).

However, one prefers to iterate the Dyson equation of equation (48) since this form has been implemented in many computer codes. Therefore, we propose an alternative scheme that also converges to the physical solution for all v and entails only a small modification of these codes. The small modification consists of iterating equation (61) for fixed W according to

$$G_{n+1} = [G_{H,n}^{-1} - iG_nW]^{-1} \quad (68)$$

and when convergence is reached for G update W according to

$$W = [1 + iv_cG_\infty G_\infty]^{-1}v_c, \quad (69)$$

where G_∞ represents the converged G for fixed W . Then reiterate equation (68) with W obtained from equation (69), etc, until convergence for both G and W is achieved. In the one-point model this scheme will also lead to the exact GW solution for all v . Finally, we note that in the absence of analytical results there does not yet exist a general strategy which permits one to know whether the converged result of a given iteration scheme corresponds to a physical or a nonphysical solution. Therefore, the study of models for which analytical results exist give important insights on how to solve this problem.

4.2. $GW\Gamma$

To obtain higher-order approximations of the Green's function y it is convenient to combine equations (28)–(31). Thus we obtain the following expression for the self-energy of the n th iteration of Hedin's equations,

$$s_{xc}^{(n)}(y) = \frac{\lambda vy}{1 + y^2 \left(v - \frac{ds_{xc}^{(n-1)}}{dy} \right)}. \quad (70)$$

We see that the self-energy of the n th iteration requires the derivative of the self-energy of the $(n - 1)$ th iteration. For example, setting $n = 1$ (with $s_{xc}^{(0)} = 0$) leads to the GW self-energy given in equation (47). We can then insert $s_{xc}^{(n)}$ in the Dyson equation (27) (for $z = 0$) to obtain the n th order approximation to y ,

$$y^{(n)} = \frac{y_0^0}{1 + y_0^0vy^{(n)} - y_0^0s_{xc}^{(n)}}, \quad (71)$$

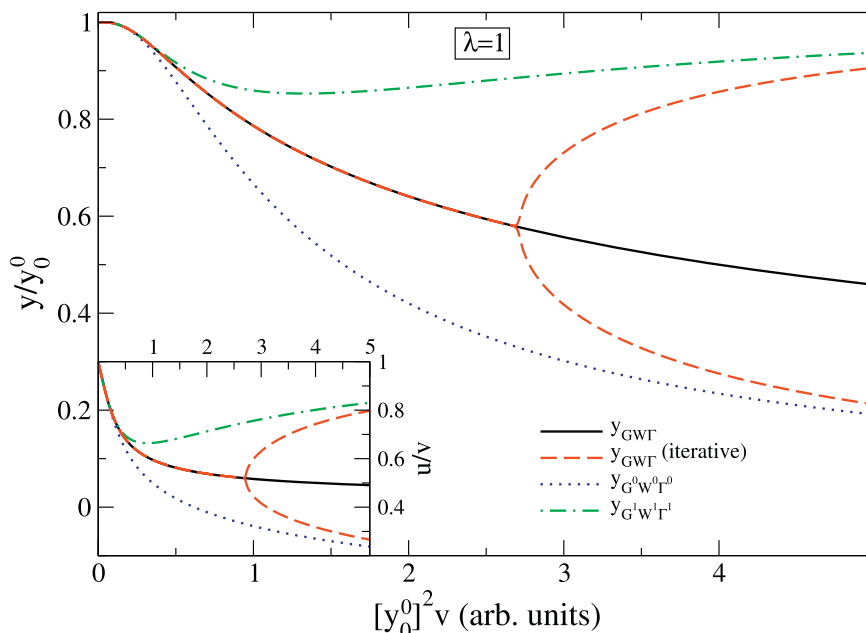


Figure 8. The $GW\Gamma$ Green's function in one point as a function of the interaction $[y_0^0]^2 v$ ($\lambda = 1$). Continuous line (black): the physical solution $y_{GW\Gamma}/y_0^0$; dashed line (red): the iterative $GW\Gamma$ result (see main text for details); dotted line (blue): $y_{G^0 w^0 \Gamma^0}/y_0^0$; dot-dashed line (green): $y_{G^1 w^1 \Gamma^1}/y_0^0$. Inset: the screened interaction $u_{GW\Gamma}/v$ as a function of the interaction $[y_0^0]^2 v$.

where we used equation (19). We therefore have to solve the following nonlinear equation

$$y_0^0 v [y^{(n)}]^2 + [1 - y_0^0 s_{xc}^{(n)}] y^{(n)} - y_0^0 = 0. \quad (72)$$

The s_{xc} obtained from a second iteration of Hedin's equations is given by

$$s_{xc}^{(2)} = \frac{\lambda v y (1 + v y^2)^2}{1 + (3 - \lambda) v y^2 + (3 + \lambda) v^2 y^4 + v^3 y^6}. \quad (73)$$

With this self-energy we will obtain the direct solutions of equation (72) as well as its iterative solution using equation (71) in the next two subsections.

4.2.1. Exact solution. Substitution of equation (73) into equation (72) leads to the following 8th-order polynomial equation for $y^{(2)}$,

$$y_0^0 - y + 2y_0^0 v y^2 - (3 - \lambda) v y^3 + 4\lambda y_0^0 v^2 y^4 - (3 + \lambda) v^2 y^5 - 2y_0^0 v^3 y^6 - v^3 y^7 - y_0^0 v^4 y^8 = 0 \quad (74)$$

where, for notational convenience, we dropped the superscript (2). The above equation for $y^{(2)}$ cannot be solved analytically. We can, however, solve it numerically for any given value of v .

We obtain eight solutions of which only one tends to y_0^0 in the limit $v \rightarrow 0$. This is the physical solution $y_{GW\Gamma}$. The remaining seven solutions are nonphysical solutions which diverge in the limit $v \rightarrow 0$. In figures 1 and 2 we compare $y_{GW\Gamma}$ to the exact Green's functions, the

approximate Green's functions obtained with the approximate solution of the linearized KBE and the GW Green's function. For $\lambda = 1$ we see that y_{GWT} provides a slight improvement over y_{GW} , in particular for weak interactions. However, in the case $\lambda = \frac{1}{2}$, y_{GW} and y_{GWT} are almost identical for all values of $[y_0^0]^2 v$. We conclude that in one point the iteration of Hedin's equations will, at best, converge very slowly.

Finally, in figures 3 and 4 we compare u_{GWT} , given by

$$u_{GWT} = v \frac{1 + (2 - \lambda)v y_{GWT}^2 + (1 + \lambda)v^2 y_{GWT}^4}{1 + (3 - \lambda)v y_{GWT}^2 + (3 + \lambda)v^2 y_{GWT}^4 + v^3 y_{GWT}^6}, \quad (75)$$

to the exact screening, to u_{lin}^0 and to u_{GW} . We see that for $\lambda = \frac{1}{2}$ the GWT screening provides the best approximation to the exact screening for small interactions.

4.2.2. Iterative solution. The GWT Dyson equation can be rewritten in even more ways than the GW Dyson equation and therefore a large number of iteration schemes are possible. Here we will report the results of the iteration scheme that is similar to the most common GW iteration scheme given in equation (61), i.e.,

$$G_{n+1} = \left[G_{H,n}^{-1} - iG_n W_n \Gamma_n \right]^{-1}. \quad (76)$$

In the one-point model this iteration scheme corresponds to

$$y_{n+1} = \left[y_0^0 \left(1 + (3 - \lambda)v y_n^2 + (3 + \lambda)v^2 y_n^4 + v^3 y_n^6 \right) \right] / \left[1 + (1 - \lambda)y_0^0 v y_n + (3 - \lambda)v y_n^2 + 3(1 - \lambda)y_0^0 v^2 y_n^3 + (3 + \lambda)v^2 y_n^4 + 3y_0^0 v^3 y_n^5 + v^3 y_n^6 + y_0^0 v^4 y_n^7 \right]. \quad (77)$$

In figure 8 we compare the results obtained with this iteration scheme to the physical GWT solution for $\lambda = 1$. Once more we observe that the iterative result does not converge to the physical solution beyond a certain interaction strength. As for GW it oscillates between two values. Moreover, compared to the iterative GW result, the range over which the iteration scheme converges to the physical solution is reduced by about 30%. We have obtained similar results for $\lambda = \frac{1}{2}$. This seems to indicate that using a more complex self-energy reduces the convergence range. In other words, beyond GW the choice of the iteration scheme becomes more crucial.

5. Conclusions

We solved the KBE in one point. We obtained a family of solutions and we showed that only one is a physical solution. Moreover, we presented a strategy to obtain the physical solution that is, in principle, not limited to the one-point model.

We showed that in the one-point model the physical solution is equal to the noninteracting solution. This is due to the fact that the terms in the KBE that contain the interaction cancel. Therefore, we proposed a slightly modified KBE in which this cancelation is partial, just as in the full functional problem. We also solved this DE and found its unique physical solution.

We assessed the accuracy of an approximate linearized KBE that lies at the heart of the GW +cumulant method. We compared it to the exact physical solution of the full KBE in one point as well as to standard approximations such as GW . The solutions of the linearized KBE are nearly exact for small interactions but deviate from the exact results for larger interactions. We showed that the solution of the linearized KBE can be improved by employing an RPA screened interaction. Adding low order vertex corrections does not seem to lead to significant improvement.

Much of the results are governed by the structure of the equations, which is the same in the one-point model and in real systems. One can hence extrapolate the findings, as long as one is careful not to over-interpret. Of course, important questions such as the position of poles corresponding to excitation energies can by definition not be treated in the one-point model.

Finally, we demonstrated that by iterating the GW Dyson equation in the usual way one does not always converge to a GW solution. We proposed a practical iterative scheme that leads to the physical GW solution for all interaction strengths.

Acknowledgments

The research leading to these results has received funding from the European Research Council under the European Union's Seventh Framework Programme (FP/2007-2013) / ERC grant agreement no. 320971. Discussion within the Collaboration Team on Correlation of the European Theoretical Spectroscopy Facility (ETSF) is greatly acknowledged. BSM acknowledges the Laboratoire des Solides Irradiés (Ecole Polytechnique, Palaiseau, France) for the support and hospitality during a sabbatical year. BSM acknowledges partial support from CONACYT-México Grant 153930.

Appendix A. Solving the KBE in one point

In this appendix we solve the KBE in one point given in equation (5) for $\lambda = 1$ and $\lambda = \frac{1}{2}$. Using the substitution $x = z - \frac{1}{y_0}$ we can rewrite equation (5) as a Riccati equation:

$$y'(x) = \frac{1}{\lambda} \left[y^2(x) - \frac{x}{v} y(x) - \frac{1}{v} \right]. \quad (\text{A.1})$$

We will now address the two cases, $\lambda = 1$ and $\lambda = \frac{1}{2}$.

A.1. General solution for $\lambda = 1$

For $\lambda = 1$ equation (A.1) becomes

$$y'(x) = y^2(x) - \frac{x}{v} y(x) - \frac{1}{v}. \quad (\text{A.2})$$

The general solution of a Riccati equation can be found if a particular solution is known. A particular solution of this Riccati equation is $y_p(x) = -\frac{1}{x}$ as can be verified by substitution. We can now transform this nonlinear DE into a linear DE by defining the function $w(x)$

according to

$$y(x) = y_p(x) + \frac{1}{w(x)} = -\frac{1}{x} + \frac{1}{w(x)}. \quad (\text{A.3})$$

Substitution of the above expression in equation (A.2) and rearranging leads to the following linear DE for $w(x)$:

$$w'(x) = \frac{x^2 + 2v}{xv}w(x) - 1. \quad (\text{A.4})$$

The solution of the homogeneous equation corresponding to the above equation is $w(x) = Kx^2e^{x^2/2v}$ with K a constant. We can then vary the constant to obtain the solution of the inhomogeneous equation. It is given by

$$w(x) = x + x^2e^{\frac{x^2}{2v}} \left(\sqrt{\frac{\pi}{2v}} \operatorname{erf} \left[\frac{x}{\sqrt{2v}} \right] + \frac{1}{C(v, y_0^0)} \right), \quad (\text{A.5})$$

where $C(v, y_0^0)$ is a function that could depend on both y_0^0 and v . Plugging this result into equation (A.3) and substituting $x = z - 1/y_0^0$ leads to the general solution given in equation (6).

A.2. General solution for $\lambda = \frac{1}{2}$

For $\lambda = \frac{1}{2}$ equation (A.1) becomes

$$y'(x) = 2y^2(x) - \frac{2x}{v}y(x) - \frac{2}{v}. \quad (\text{A.6})$$

To solve the above equation we first rewrite this nonlinear first-order DE as a linear second-order DE by defining the function $u(x)$ as

$$y(x) = -\frac{u'(x)}{2u(x)}. \quad (\text{A.7})$$

We can thus rewrite equation (A.6) according to

$$u''(x) + p(x)u'(x) + q(x)u(x) = 0 \quad (\text{A.8})$$

with $p(x) = \frac{2x}{v}$ and $q(x) = -\frac{4}{v}$. A particular solution of this second-order DE is

$$u_1(x) = \frac{v + 2x^2}{v} \quad (\text{A.9})$$

which can be verified by substitution into equation (A.8). A second independent solution is then given by [19]

$$u_2(x) = u_1(x) \int^x dt \frac{1}{u_1^2(t)} e^{-\int^t p(s) ds} \quad (\text{A.10})$$

$$= (v + 2x^2) \left[\frac{xe^{-\frac{x^2}{v}}}{2v + 4x^2} + \frac{1}{4} \sqrt{\frac{\pi}{v}} \operatorname{erf} \left[\frac{x}{\sqrt{v}} \right] \right]. \quad (\text{A.11})$$

The general solution for $u(x)$ can therefore be written as

$$u(x) = C_1(v + 2x^2) \left[\frac{xe^{-\frac{x^2}{v}}}{2v + 4x^2} + \frac{1}{4} \sqrt{\frac{\pi}{v}} \operatorname{erf} \left[\frac{x}{\sqrt{v}} \right] + \frac{C_2}{v} \right], \quad (\text{A.12})$$

where for notational convenience we have suppressed the dependence of C_1 and C_2 on v and y_0^0 . The derivative of $u(x)$ is given by

$$u'(x) = C_1 \left[e^{-\frac{x^2}{v}} + x \sqrt{\frac{\pi}{v}} \operatorname{erf} \left[\frac{x}{\sqrt{v}} \right] + \frac{4x}{v} C_2 \right]. \quad (\text{A.13})$$

Substituting these results into equation (A.7) then leads to the general solution for $y(x)$

$$y(x) = - \frac{e^{-\frac{x^2}{v}} + x \sqrt{\frac{\pi}{v}} \operatorname{erf} \left[\frac{x}{\sqrt{v}} \right] + \frac{4x}{v} C_2}{\left[xe^{-\frac{x^2}{v}} + \left(x^2 + \frac{v}{2}\right) \left(\sqrt{\frac{\pi}{v}} \operatorname{erf} \left[\frac{x}{\sqrt{v}} \right] + \frac{4}{v} C_2 \right) \right]} \quad (\text{A.14})$$

$$= - \left[x + \frac{v}{2x} \left[1 + \frac{1}{\sqrt{\frac{\pi}{v}} x e^{\frac{x^2}{v}} \left[\operatorname{erf} \left[\frac{x}{\sqrt{v}} \right] + \frac{1}{C(v, y_0^0)} \right]} \right] \right]^{-1}, \quad (\text{A.15})$$

where we defined

$$C(v, y_0^0) = \frac{\sqrt{v\pi}}{4C_2(v, y_0^0)}. \quad (\text{A.16})$$

Substituting $x = z - \frac{1}{y_0^0}$ leads to equation (11).

Appendix B. Hedin's equations in one point

In analogy with the full functional problem we can define the exchange–correlation part of the self-energy $s_{xc}(y)$ in one point as

$$s_{xc}(y) = \lambda v \frac{y'(z)}{y(z)}. \quad (\text{B.1})$$

The KBEs in equations (5) and (15) can then be rewritten as Dyson equations:

$$y(z) = y_0^0 + y_0^0 z_{\text{tot}}(z) y(z) + y_0^0 s_{xc}(y) y(z), \quad (\text{B.2})$$

$$y(z) = y_H(z) + y_H(z) z y(z) + y_H(z) s_{xc}(y) y(z), \quad (\text{B.3})$$

where $z_{\text{tot}}(z) = z - v y(z)$, which represents the total classical potential in one point. Using the chain rule we can rewrite $s_{xc}(y)$ defined in equation (B.1) according to

$$s_{xc}(y) = \lambda v \frac{1}{y(z)} \frac{dy(z_{\text{tot}}(z))}{dz_{\text{tot}}} \frac{dz_{\text{tot}}}{dz} = \lambda \frac{u(z) \tilde{p}(z)}{y(z)}, \quad (\text{B.4})$$

where we used equations (20), (21), and (24) and where we defined

$$\tilde{p}(z) = \frac{dy(z_{\text{tot}}(z))}{dz_{\text{tot}}} \quad (\text{B.5})$$

which represents the irreducible polarizability in one point.

The irreducible polarizability is related to the reducible polarizability of equation (21) by

$$\tilde{p}(z) = p(z) + p(z)v\tilde{p}(z). \quad (\text{B.6})$$

which can be verified by applying the chain rule to equation (B.5). The screened interaction $u(z)$ defined in equation (24) can be rewritten in terms of $\tilde{p}(z)$ with the help of equation (B.6):

$$u(z) = \frac{v}{1 + v\tilde{p}(z)} = v - v\tilde{p}(z)u(z). \quad (\text{B.7})$$

The irreducible polarizability can be rewritten as

$$\tilde{p}(z) = \frac{dy}{dz_{\text{tot}}} = -y^2 \frac{dy^{-1}}{dz_{\text{tot}}} = y^2 \tilde{g}(y), \quad (\text{B.8})$$

where $\tilde{g}(y)$ represents the irreducible vertex function in one point:

$$\tilde{g}(y) = -\frac{dy^{-1}}{dz_{\text{tot}}}. \quad (\text{B.9})$$

For notational convenience we have suppressed the dependence of y on $(z_{\text{tot}}(z))$ in the above expressions. We will continue to do so in the remainder of this section. With the help of equation (B.8) we can now rewrite the self-energy given in equation (B.4) as

$$s_{\text{xc}}(y) = \lambda y(z)u(z)\tilde{g}(z). \quad (\text{B.10})$$

Dividing both sides of equation (B.2) by $y_0^0 y(z)$ and differentiating with respect to z_{tot} leads to

$$0 = \frac{dy^{-1}}{dz_{\text{tot}}} + 1 + \frac{ds_{\text{xc}}(y)}{dz_{\text{tot}}} = -\tilde{g}(y) + 1 + \frac{ds_{\text{xc}}(y)}{dy} y^2 \tilde{g}(y), \quad (\text{B.11})$$

where we used equations (B.5), (B.8), and (B.9). This expression can be rewritten as

$$\tilde{g}(y) = 1 + \frac{ds_{\text{xc}}(y)}{dy} y^2 \tilde{g}(y). \quad (\text{B.12})$$

The expressions given in equations (B.3), (B.7), (B.8), (B.10), and (B.12) constitute Hedin's equations in one point.

Appendix C. Solution of a modified KBE in one point

In this appendix we investigate a slightly modified set of Hedin's equations in one point that was introduced by Molinari *et al* to count diagrams [12, 13]. The modification is in the irreducible polarization given in equation (30) to which they added a minus sign, i.e., $\tilde{p} = -y^2 \tilde{g}$. Pavlyukh and Hübner solved this set of equations (for $z = 0$) and found an implicit solution for y [14]. In the next two subsections we show how to obtain an explicit solution and how to determine the physical solution.

C.1. General solution

We can find an explicit solution for these modified Hedin's equations by realizing that it is equivalent to the solution of the KBE in the limit of vanishing φ if we modify the KBE given in (3) in the following way,

$$y(z) = y_0^0 + \nu y_0^0 y^2(z) + y_0^0 z y(z) + \nu y_0^0 y'(z), \quad (\text{C.1})$$

i.e., we added a minus sign to the quadratic term which represents the Hartree contribution in one point.

The solution of the modified KBE in equation (C.1) is given by

$$y(z) = \frac{1}{\nu y_0(z)} + \left[e^{-\frac{1}{2\nu y_0^2(z)} \sqrt{-\frac{\nu\pi}{2}}} \left(\operatorname{erf} \left[\frac{-1}{\sqrt{-2\nu y_0^2(z)}} \right] + C(\nu, y_0^0) \right) \right]^{-1}, \quad (\text{C.2})$$

where $C(\nu, y_0^0)$ is a function that could depend on both ν and y_0^0 . The derivation of this result can be found in appendix D. This explicit solution of the modified KBE is equivalent to the implicit solution of the modified Hedin's equations obtained by Pavlyukh and Hübner for the case $z = 0$. Their implicit solution can be obtained by setting $z = 0$ in equation (C.2) followed by the substitution $y_0^0 = \frac{y_H^0}{1 + \nu y_H^0 y(z=0)}$.

C.2. Physical solution

To obtain the physical solution we investigate equation (C.2) in the limit $\nu \rightarrow 0$ in which $y(z)$ should reduce to $y_0(z)$ for any z . As a first step we will determine $C(\nu = 0, y_0^0)$ by studying potentials z for which $|y_0^2(z)| < 0$. We use the asymptotic expansion of the error function given in equation (7) to rewrite $y(z)$ given in equation (C.2) as

$$y(z) = \frac{1}{\nu y_0(z)} + \left[e^{\frac{1}{2\nu |y_0^2(z)|} \sqrt{-\frac{\nu\pi}{2}}} \left(1 + C(\nu, y_0^0) - \sum_{n=0}^{\infty} (2n-1)!! \nu^{n+1} y_0^{2n+1}(z) \right) \right]^{-1}. \quad (\text{C.3})$$

In the limit $\nu \rightarrow 0^+$ the first term on the right-hand will tend to $\mp i\infty$ while the second term on the right-hand side will tend either to zero (for $C(\nu = 0, y_0^0) \neq -1$) or to $\pm i\infty$ (for $C(\nu = 0, y_0^0) = -1$). This means that $y(z)$ will tend to $\mp i\infty$ for any $C(\nu = 0, y_0^0) \neq -1$. In the case $C(\nu, y_0^0) = -1$ we can rewrite the above expression as

$$y(z) = \frac{y_0(z) + \sum_{n=1}^{\infty} (2n+1)!! \nu^n y_0^{2n+1}(z)}{1 + \sum_{n=1}^{\infty} (2n-1)!! \nu^n y_0^{2n}(z)}. \quad (\text{C.4})$$

We see that in the limit $\nu \rightarrow 0$ we obtain the noninteracting solution $y_0(z)$. We conclude that $C(\nu = 0, y_0^0) = -1$ corresponds to the physical solution.

In order to determine $C(\nu, y_0^0)$ for finite ν we assume that $C(\nu, y_0^0)$ has a Taylor expansion around $\nu = 0$. Then, for $y_0^2(z) < 0$, in the limit $\nu \rightarrow 0^+$ the right-hand side of equation (C.3)

tends to $y_0(z)$ if and only if all the coefficients of the Taylor expansion of $C(v, y_0^0)$ vanish except the first. We conclude that $C(v, y_0^0) = -1$ for all v . Therefore the physical solution is given by

$$y(z) = \frac{1}{vy_0(z)} - \left[e^{-\frac{1}{2vy_0^2(z)}\sqrt{-v\pi}} \left(\operatorname{erf} \left[\frac{1}{\sqrt{-2vy_0^2(z)}} \right] + 1 \right) \right]^{-1}. \quad (\text{C.5})$$

The solution for $z = 0$ becomes

$$y_v = \frac{1}{y_0^0 v} - \left[e^{-\frac{1}{2v[y_0^0]^2}\sqrt{-v\pi}} \left(\operatorname{erf} \left[\frac{1}{\sqrt{-2v[y_0^0]^2}} \right] + 1 \right) \right]^{-1}. \quad (\text{C.6})$$

Appendix D. General solution of the modified KBE

In this section we solve the modified KBE given in equation (C.1). Using a change of variable $x = z - 1/y_0^0$ the modified KBE in equation (C.1) can be rewritten as

$$-y'(x) = y^2(x) + \frac{x}{v}y(x) + \frac{1}{v}. \quad (\text{D.1})$$

A particular solution of this Riccati equation is $y(x) = -\frac{x}{v}$ as can be verified by substitution. We now write the general solution in the form $y(x) = -\frac{x}{v} + \frac{1}{w(x)}$. Substitution in equation (D.1) leads to the following linear DE

$$w'(x) = -\frac{x}{v}w(x) + 1. \quad (\text{D.2})$$

The solution of this linear DE is

$$w(x) = e^{-\frac{x^2}{2v}} \left(\sqrt{-\frac{v\pi}{2}} \operatorname{erf} \left[\frac{x}{\sqrt{-2v}} \right] + \tilde{C}(v, y_0^0) \right), \quad (\text{D.3})$$

where $\tilde{C}(v, y_0^0)$ is a function that could depend on both v and y_0^0 . The general solution for $y(x)$ therefore becomes

$$y(x) = -\frac{x}{v} + \left[e^{-\frac{x^2}{2v}} \sqrt{-\frac{v\pi}{2}} \left(\operatorname{erf} \left[\frac{x}{\sqrt{-2v}} \right] + C(v, y_0^0) \right) \right]^{-1}, \quad (\text{D.4})$$

where we defined $C(v, y_0^0) = \sqrt{-\frac{2}{v\pi}} \tilde{C}(v, y_0^0)$. Substituting $x = z - \frac{1}{y_0^0}$ leads to equation (C.2).

References

- [1] Hedin L 1965 *Phys. Rev.* **139** A796
- [2] Lani G, Romaniello P and Reining L 2012 *New J. Phys.* **14** 013056
- [3] Aryasetiawan F, Hedin L and Karlsson K 1996 *Phys. Rev. Lett.* **77** 2268

- [4] Guzzo M, Lani G, Sottile F, Romaniello P, Gatti M, Kas J J, Rehr J J, Silly M G, Sirotti F and Reining L 2011 *Phys. Rev. Lett.* **107** 166401
- [5] Lischner J, Vigil-Fowler D and Louie S G 2013 *Phys. Rev. Lett.* **110** 146801
- [6] Guzzo M, Kas J J, Sponza L, Giorgetti C, Sottile F, Pierucci D, Silly M G, Sirotti F, Rehr J J and Reining L 2014 *Phys. Rev. B* **89** 085425
- [7] Kas J J, Rehr J J and Reining L 2014 *Phys. Rev. B* **90** 085112
- [8] Aulbur W G, Jönsson L and Wilkins J W 2000 *Solid State Physics* vol 54 (New York: Academic) p 1
- [9] Aryasetiawan F and Gunnarsson O 1998 *Rep. Prog. Phys.* **61** 237
- [10] Mahan G D and Sernelius B E 1989 *Phys. Rev. Lett.* **62** 2718
- [11] Shirley E L 1996 *Phys. Rev. B* **54** 7758
- [12] Molinari L G 2005 *Phys. Rev. B* **71** 113102
- [13] Molinari L G and Manini N 2006 *Eur. Phys. J. B* **51** 331
- [14] Pavlyukh Y and Hübner W 2007 *J. Math. Phys.* **48** 052109
- [15] Tandetzky F, Dewhurst J K, Sharma S and Gross E K U 2012 arXiv:1205.4274
- [16] Rostgaard C, Jacobsen K W and Thygesen K S 2010 *Phys. Rev. B* **81** 085103
- [17] Caruso F, Rinke P, Ren X, Scheffler M and Rubio A 2012 *Phys. Rev. B* **86** 081102
- [18] Caruso F, Rinke P, Ren X, Rubio A and Scheffler M 2013 *Phys. Rev. B* **88** 075105
- [19] Kamke E 1977 *Differentialgleichungen: Lösungsmethoden und Lösunge, I, Gewöhnliche Differentialgleichungen* (Leipzig: Teubner)